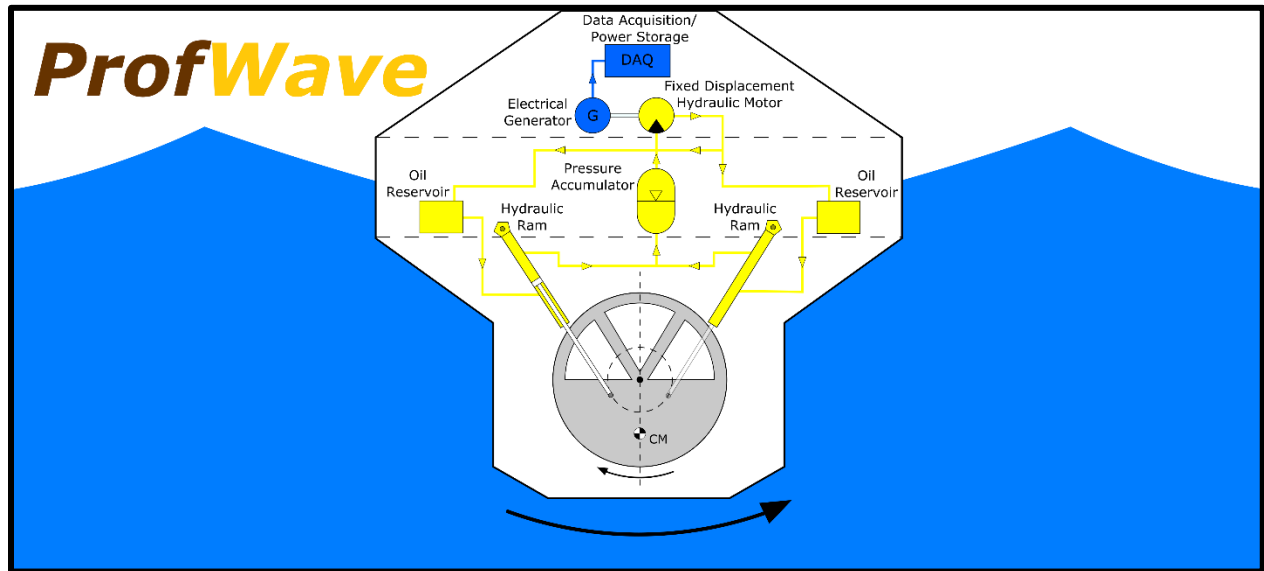


ProfWave: An Ocean Wave Energy Converter

Logan Greer, Joseph Mandara, Aaron Sorin, Richard Sbresny
Rowan University, Mechanical Engineering



Abstract

This Rowan University Junior/Senior Engineering Clinic project seeks to develop a medium-scale ocean wave energy converter (WEC) that is capable of producing power from the motion of the waves. This semester, the team secured funding for the project via PROFunder (Rowan's crowdfunding campaign) and evaluated potential testing locations. A buoy-pendulum design was selected and attempts were made to dynamically model and simulate the system's motion. Prototypes of the WEC's hull were 3D printed and tested, and preliminary designs of the internal power production and data acquisition systems were completed. Next semester, the WEC's design will be optimized for manufacturability, cost, and efficiency, then constructed and tested in a local body of water.

Table of Contents

| | | |
|-----|--|----|
| 1 | Introduction | 1 |
| 1.1 | Ocean Wave Energy Background | 1 |
| 1.2 | Project Goals and Timeline | 1 |
| 1.3 | Acquiring Funding | 2 |
| 1.4 | Potential Testing Locations | 2 |
| 2 | ProfWave Design Details | 3 |
| 2.1 | Design Selection and Overview | 3 |
| 2.2 | Mathematical Model | 6 |
| 2.3 | External Mechanical Design | 7 |
| 2.4 | Internal Mechanical Design | 12 |
| 2.5 | Power Take-Off System | 15 |
| 2.6 | Electronics and Data Acquisition | 17 |
| 3 | Technological Impact Statement | 20 |
| 3.1 | Societal Impact | 20 |
| 3.2 | Environmental Impact | 20 |
| 3.3 | Manufacturability | 20 |
| 4 | Conclusion | 21 |
| 5 | Acknowledgments | 22 |
| 6 | References | 22 |
| 7 | Appendix | 23 |
| 7.1 | Fall 2016 Project Gantt Chart | 23 |
| 7.2 | Wave Data Collected for Pierce’s Point, NJ | 24 |
| 7.3 | GPIO Pinout of Raspberry Pi 3 Model B | 25 |
| 7.4 | Connection Diagram for ADS1115 16-Bit ADC | 25 |
| 7.5 | Connection Diagram for ADXL345 Digital Accelerometer | 25 |

1 Introduction

1.1 Ocean Wave Energy Background

With the world's population – and its energy needs – continuing to grow, the development of alternative, sustainable forms of energy is becoming increasingly important in order to conserve fossil fuel resources and reduce the emissions from their use in power generation [1]. Fossil fuels are finite resources, and their environmental costs have been rising considerably over the past few decades, a trend that has sparked new interest in the research and development of renewable energy technologies [2]. Various forms of solar, wind, and crop-based energy have been studied and developed in order to provide alternate forms of renewable energy; however, in recent years, scientists have begun to look more closely at the ocean as a new source of untapped energy potential [3]. Covering over 70% of the Earth, the ocean – specifically ocean waves – offers an enormous and continuous source of energy that is renewable, environmentally friendly, and readily available near the majority of the world's most populated areas [4].

There are a number of different ways that ocean wave energy can be harnessed, and so the research and development taking place spans a variety of different wave energy conversion technologies. In general, the conversion of ocean wave energy into useable electrical energy begins with a wave energy converter (WEC), a device that can either float on the ocean surface or rest under the surface, tethered to the ocean floor [4]. The WEC converts the oscillatory motion of wave energy into translational and/or rotational mechanical energy, after which a power take-off system (PTO) converts this mechanical energy into electrical energy that is distributed across a power grid [5]. WECs are typically classified in one of two ways: by deployment location – shoreline (fixed to the shoreline or shallow ocean floor), near-shore (depths between ten and twenty meters), or offshore (depths greater than forty meters) – or by the type of device and mode of operation [2]. The latter method lends itself to a more thorough look specifically at the engineering and technology behind WEC devices and their designs, but the two are often interconnected. This paper will document the progress of a new academic project at Rowan University that is centered on developing a WEC that is based on an unconventional design and designed for operation in shallow water.

1.2 Project Goals and Timeline

This new Junior/Senior Engineering Clinic project was developed by students at the end of the summer in order to explore the potential of ocean wave energy by developing a medium-scale WEC (constrained to a five-foot cube of space) during the 2016-2017 academic year.

ProfWave's overall goal is to develop a WEC that can produce enough power to be net positive (i.e. generate more power than is required for operation). To accomplish this goal, the team established a timeline of key intermediate goals for each semester. The Fall 2016 Semester focused on securing funding for the project, completing the preliminary WEC design, and investigating potential testing locations. The Spring 2017 Semester will focus on completing the final WEC design, obtaining any necessary testing permission, fabricating the WEC, and ultimately testing and evaluating its performance. The team then developed a Gantt chart to outline the tasks, bi-weekly schedule, and team member assignments needed to accomplish the fall semesters goals. This Gantt chart can found in the attached Appendix.

1.3 Acquiring Funding

Since ProfWave is a new clinic project, it had no budget at the start of the fall semester. Looking ahead and recognizing that the project cannot be taken from design to fabrication to testing without the means to buy materials and parts and pay for transportation and testing costs, the team's primary concern after establishing an organizational structure and timeline was to obtain funding. At the beginning of the semester, the team submitted a funding proposal to the Rowan University Mechanical Engineering Department and was awarded \$300. The team also applied in September to the Rowan University Alumni Association's fall PROffunder campaign, which is the university's equivalent of a crowdfunding campaign for student projects and events.

Applying to PROffunder requires the submission of a detailed proposal that outlines the following: the organization under which the project is being completed; a team of at least three members who will be working on the project; a faculty representative; two alumni sponsors; a description of the project; a social media and advertising plan; fundraising goals; implementation plans for money raised; and project "stretch" goals. ProfWave was selected as one of ten projects to be featured in the fall PROffunder campaign. The campaign ran from November 1st to November 30th, and ProfWave was able to successfully raise \$2,451, which will help pay for a significant portion of the project's upcoming expenses.

1.4 Potential Testing Locations

In order to evaluate the WEC's effectiveness at generating power, it will need to be tested in one of the nearby bodies of water. Several locations were considered, including the Northern Chesapeake Bay, the Barnegat Bay, the Delaware Bay, and the Atlantic Ocean. Locations were evaluated based on the following criteria: water depth, typical wave height, presence of high-traffic boating lanes, and proximity to boating facilities (docks, marinas, etc.). The Atlantic was ruled out early on in the investigation, for it was deemed too susceptible to unpredictable wave patterns. The Northern Chesapeake Bay was deemed unsuitable due to a lack of sufficient water depth. A minimum depth of ten feet was deemed to be sufficient for safe operation of the WEC, and while there are a few locations in the Northern Chesapeake that meet this criteria, they are all located in high-traffic boating channels. Further, the waters of the Northern Chesapeake tend to be calm, which is not ideal as the WEC's power generation is dependent on wave height. The Barnegat Bay was also excluded for similar reasons. The Delaware Bay, however, was identified as ideal due to its easily attainable depths of greater than ten feet that are close to shore and not within existing boating lanes.

Now focusing the investigation on the Delaware Bay, several areas north of Cape May, NJ were evaluated. Pierce's Point was selected as the best available location for the following reasons: water depth is sufficient, wave height and period data is available (SwellInfo.com) and promising (heights average between one and two feet), and there are no nearby boating lanes. Also, Rutgers University has a Cape Shore Laboratory located less than a mile to the south of Pierce's Point that may be able to provide the team with helpful information about the nearby area and waters and potentially even assist with transporting the WEC to its drop site. Contact with the director of the laboratory has been made, and hopefully continued communication will prove useful moving forward with test planning.

Lastly, the team recently discovered the Ohmsett test facility (Leonardo, NJ), which is the largest outdoor saltwater wave tank in North America. Though primarily used for testing oil spill response equipment, the facility has recently expanded its mission to offer a testing venue for wave energy conversion devices. In the near future, the team will seek to make contact with the Ohmsett facility to discuss the potential of scheduling a test in their wave tank. The ability to perform a test under the controlled conditions of a wave tank would be highly beneficial when evaluating the WEC's effectiveness.

2 ProfWave Design Details

Figure 2.1 provides a basis for the directional terminology used throughout this paper to describe the WEC's motion in the water.

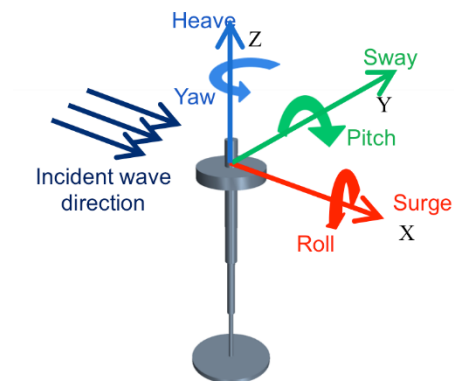


Figure 1.1.1. Directional terminology used to describe the motion of a body in water.

2.1 Design Selection and Overview

There were three different types of WEC designs that the team considered modeling ProfWave after: a single degree-of-freedom (DOF) point absorber, a submerged pressure differential design, and a buoy-pendulum design, all shown in Figs. 2.1.1, 2.1.2, and 2.1.3, respectively.

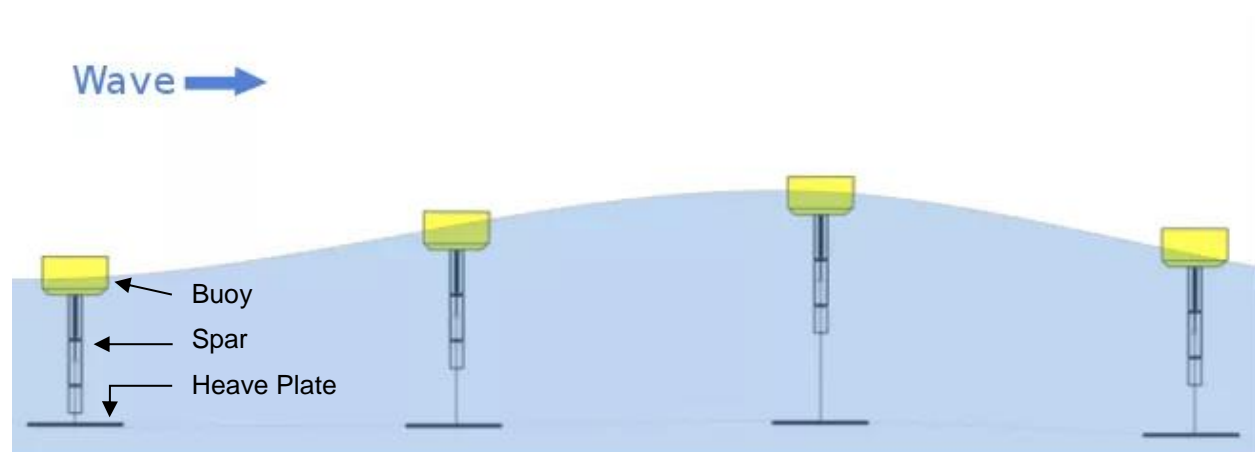


Figure 2.1.1. Operation of a single DOF point absorber.

As shown, the point absorber typically consists of two distinct bodies: a conjoined buoy and spar, and a neutrally-buoyant heave plate. The oscillatory motion of a wave gives the buoy/spar a heaving motion, in phase with the wave, while the heave plate remains stationary. This relative motion between the buoy/spar and the heave plate is what actuates the power take-off system. Since only the heaving motion is of concern, one great aspect of this design is that its orientation relative to oncoming waves does not impact its performance. While the point absorber is a relatively simple design, it has been exhaustively studied in industry and academia, and its simplicity actually makes it less interesting to study from an academic perspective. Additional pros and cons for the point absorber design are shown in Table 2.1.1.

Table 2.1.1. Design considerations for a single DOF point absorber.

| PROS | CONS |
|--|--|
| Less extensive waterproofing needed for PTO system and electronics | Requires more knowledge of testing conditions (wave depth and amplitude, weather conditions) |
| Only requires heave motion | Larger mechanical structure |
| Easier to work on once testing has begun and remove from water after testing | Heave plate needs to be neutrally buoyant |

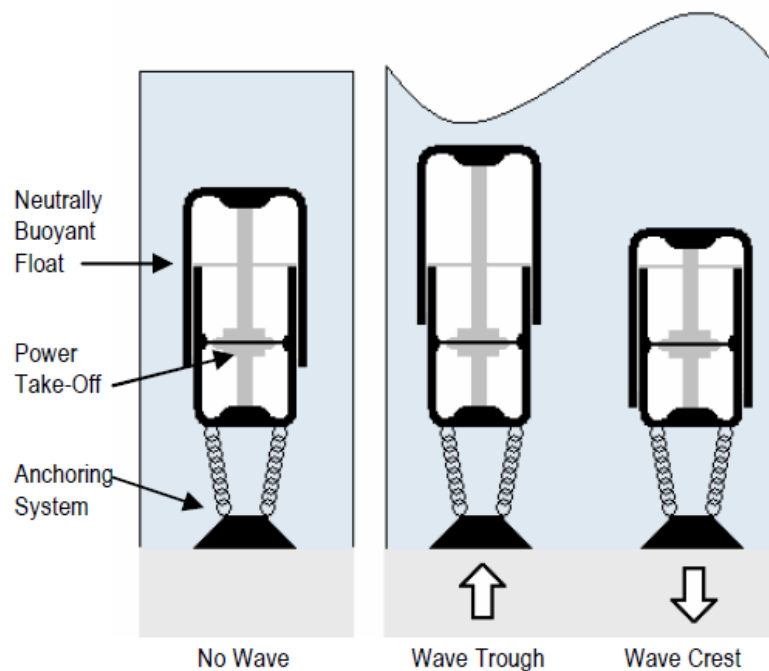


Figure 2.1.2. Operation of a submerged pressure differential WEC.

The submerged pressure differential shown in Fig. 2.1.2 above also makes use of the waves' oscillatory motion to generate power. However, unlike the point absorber, the submerged

pressure differential is moored to the bottom of the ocean (or other body of water) and uses differences in pressure to actuate its heaving motion. So, as a wave crest passes over the device, this increase in height results in an increase in water pressure acting on the device, which forces it downward. At the other extreme, when a wave trough passes over the device, there is a decrease in water height and pressure acting on the device, and so it travels upward in the direction of low pressure. While this complex method of operation makes a submerged pressure differential more interesting to study, the risks associated with submerging an on-board electronic data acquisition system in the water are much too high. Additional pros and cons for the submerged pressure differential are shown in Table 2.1.2.

Table 2.1.2. Design considerations for a submerged pressure differential WEC.

| PROS | CONS |
|---|---|
| Less dependent on amplitude of surface waves | Fully submerged PTO system and electronics requires that enclosure is completely waterproofed |
| Simpler mechanical structure (no heave plate) | Difficult remove from water after testing |
| Only float needs to be neutrally buoyant | Difficult/impossible to work on once testing has begun |

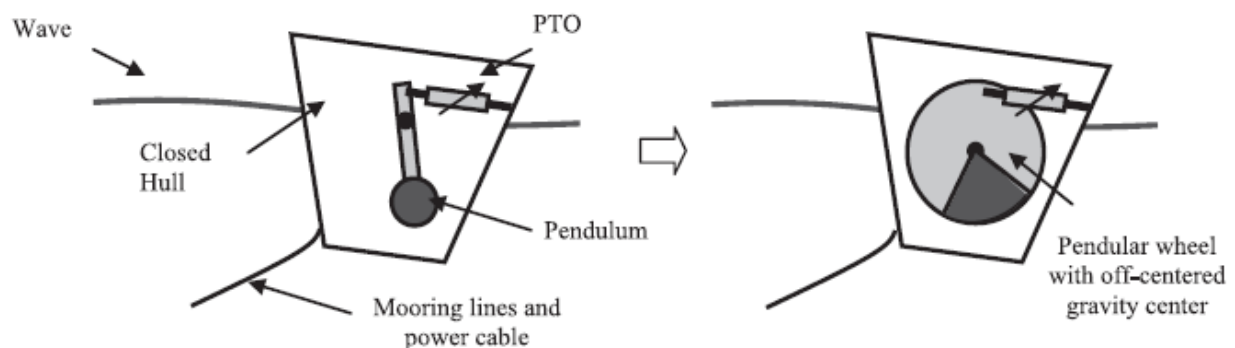


Figure 2.1.3. Operation of a buoy-pendulum WEC.

The buoy-pendulum design, which the team did choose to model ProfWave after, is shown in Fig 2.1.3 above, and functions in an entirely different method than either of the previous two designs. As shown, its two main components are a buoy, or hull, and an internal pendulum - which can be designed as a standard pendulum or a circular shape that is weighted off-center. The oscillatory motion of a wave causes the buoy and pendulum to pitch forward and backward; however, their differences in mass and moment of inertia (MoI) create a relative angular displacement between the two bodies. Attached to the pendulum are one or more hydraulic cylinders that are actuated by this relative angular displacement and drive a PTO system to generate power. While this design is more complex and typically less efficient than either of the previous two, its complex dynamics and multiple distinct subsystems made it more interesting to

study and provided ample work for each team member. Additional pros and cons for the buoy-pendulum design are shown in Table 2.1.3.

Table 2.1.3. Design considerations for a buoy-pendulum WEC.

| PROS | CONS |
|---|--|
| Simpler exterior mechanical structure | Need to control orientation relative to incident waves |
| Less extensive waterproofing needed for power generation system and electronics | More complex to model and simulate |
| Easiest to put in and remove from water after testing | Potentially less power output |
| Easier to work on once testing has begun | |

2.2 Mathematical Model

After selecting the buoy-pendulum design to model ProfWaver after, the next step in the design was to gain a better understanding of the system's physics and develop a mathematical model governing the system's motion. Obtaining a model for the motion of the buoy and pendulum centers of mass, based on various input conditions, will make it possible to calculate the important factors that control the system's power output, such as linear and angular displacement, velocity, and acceleration, and resulting forces. This knowledge can then be used to optimize the design. The system was modeled based on the diagram in Fig. 2.2.1.

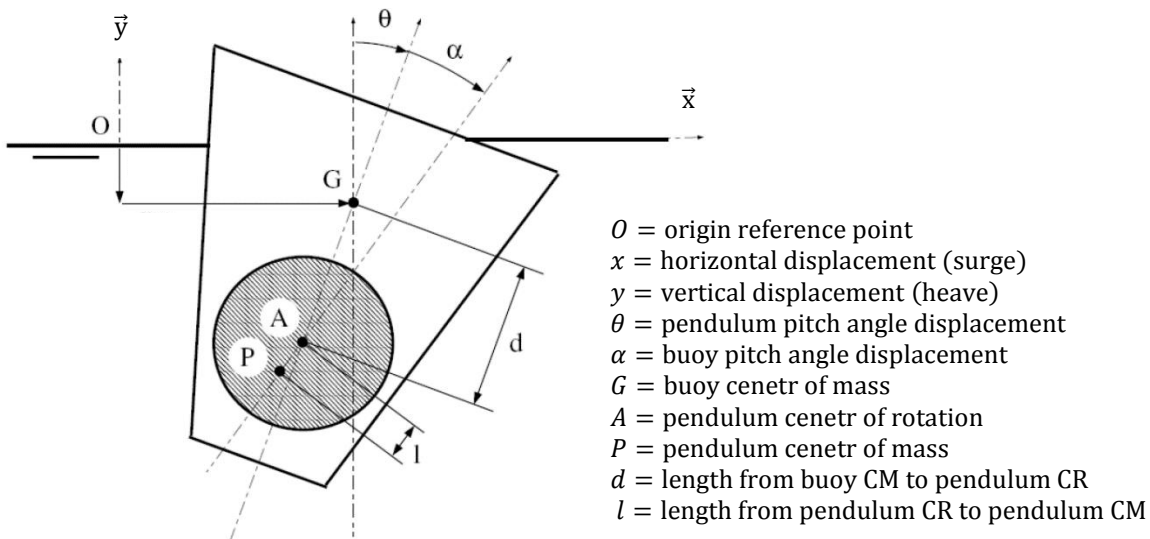


Figure 2.2.1. Buoy-pendulum design indicating key dimensions

A dynamic analysis to solve for x , y , θ , and α was then performed on the buoy and pendulum centers of mass, using Lagrangian mechanics. The Lagrange equation is given by:

$$\frac{d}{dt} \left(\frac{\partial T}{\partial \dot{q}_j} \right) - \frac{\partial T}{\partial q_j} + \frac{\partial V}{\partial q_j} = F_j \quad (2.2.1)$$

where T is kinetic energy, V is potential energy, q is the variable of interest, and F are any external forces acting on the body. After calculating the potential and kinetic energies of the buoy and pendulum centers of mass, Eq. 2.2.1 was applied with respect to each of the four variables of interest. Rearranging the resulting equations in terms equivalent to mass, acceleration, and external forces, and rewriting them in matrix notation produced the following mass, acceleration, and force matrices, respectively:

$$M = \begin{bmatrix} m_b + m_p & 0 & dm_p \cos \theta + lm_p \cos(\theta + \alpha) & lm_p \cos(\theta + \alpha) \\ 0 & m_b + m_p & dm_p \sin \theta + lm_p \sin(\theta + \alpha) & lm_p \sin(\theta + \alpha) \\ dm_p \cos \theta + lm_p \cos(\theta + \alpha) & dm_p \sin \theta + lm_p \sin(\theta + \alpha) & I_b + I_p + d^2 m_p + 2dm_p \cos \alpha & I_p + l^2 m_p + dlm_p \cos \alpha \\ lm_p \cos(\theta + \alpha) & lm_p \sin(\theta + \alpha) & I_p + l^2 m_p + dlm_p \cos \alpha & I_p + l^2 m_p \end{bmatrix}$$

$$\ddot{q} = \begin{Bmatrix} \ddot{x} \\ \ddot{y} \\ \ddot{\theta} \\ \ddot{\alpha} \end{Bmatrix}$$

$$F = \begin{bmatrix} F_x - k_x x + \dot{\theta}^2 dm_p \sin \theta + (\dot{\theta} + \dot{\alpha})^2 \sin(\theta + \alpha) \\ F_y - k_y y + \dot{\theta}^2 dm_p \cos \theta + (\dot{\theta} + \dot{\alpha})^2 \cos(\theta + \alpha) - g(m_p + m_b) \\ F_\theta - k_\tau \theta + \dot{\alpha}^2 dlm_p \sin \alpha + 2\dot{\theta}\dot{\alpha} dlm_p \sin \alpha - dgm_p \sin \theta - lgm_p \sin(\theta + \alpha) \\ F_\alpha - \dot{\theta}^2 dlm_p \sin \alpha - lgm_p \sin(\theta + \alpha) \end{bmatrix}$$

Of particular interest in this model is the force matrix, which includes external forces in the surge, heave, and pitching directions, as well as surge, heave, and pitching buoyancy. The buoyancy in the heave direction can be calculated by applying Archimedes' principle. After incorporating this buoyancy, a series of MATLAB scripts were created to solve for the displacements and velocities in the surge, heave, and pitch directions, and plot the resulting motion of the buoy and pendulum centers of mass and the pendulum center of rotation. However, accounting for the remaining external forces is a much more complicated process, and so they were set equal to zero for the time being. Additionally, while the scripts function properly, they cannot provide accurate results without true masses, moments of inertia, and dimensions for a full-scale model. As these parameters cannot be determined without a completed three-dimensional model of the WEC, the team decided to shift focus to designing the specifics of the WEC and modeling it in SolidWorks, with the caveat that some form of mathematical modeling must be completed prior to fabrication in order to estimate the system's expected power output and evaluate the design. This could also be accomplished using commercial hydrodynamic software, namely as ANSYS Aqwa, which seems to be the industry and academia standard for WEC simulation and modelling. The team is currently in contact with an ANSYS representative about acquiring access to a limited or trial version of the software package.

2.3 External Mechanical Design

Based on the different designs of buoy-pendulum WECs that were investigated, the team formed a general idea of what the final exterior should look like. It was decided that the exterior should

have two main compartments: a small, narrow lower compartment, where the swinging pendulum would be housed; and a larger, wider upper compartment, where the hydraulic and electronic systems would be housed. During this stage, the team also expected the final design to have polygonal cross-sections, when viewed from above, and eventually would decide on irregular, octagonal cross-sections for the final design. For reference, each time a cross-section is indicated throughout the remainder of this report, it is to be assumed that the viewing angle is from above.

After deciding on a general shape, the next step was to refine the design of the outer structure. Unfortunately, because the team lacked access to the proper software to test computer generated models, they decided that qualitatively analyzing prototypes with different characteristics through experimentation would be the best method for refining the design. In order for the prototypes to yield meaningful data, they needed to be appropriately scaled so that the characteristic flow around the prototypes matches the characteristic flow around the actual-size WEC. From ensuing research and published work in this area, the team determined that the best method for scaling a prototype buoy is to scale based on Froude number, the dimensionless ratio of inertial forces to gravitational forces, which is shown in Eq. 2.3.1 [6].

$$(F_r)_p = (F_r)_m \rightarrow \frac{(v_p)^2}{gL_p} = \frac{(v_m)^2}{gL_m} \quad (2.3.1)$$

Once the external design was conceptualized, the team moved into the prototyping phase of this system. The first prototype (Rev 1) was designed and modeled in SolidWorks, then saved as a stereolithography (.stl) file, and imported into Cura, a software package that is used to generate g-code files that can be read by a 3D printer. With the g-code file generated, the Rev 1 prototype was created using a 3D printer, and the team performed the first testing of the prototyping phase. This prototype was designed to have circular cross-sections and can be seen in Fig. 2.3.1.



Figure 2.3.1. Rev 1, prototype of external mechanical structure.

The prototype was purposely designed with circular cross-sections because the team planned to use the first tests as practice to determine exactly what the testing procedure would be, to decide

which qualitative metrics would be varied during subsequent design iterations, because it would be easy to quickly model, and to determine if all cross-sections with radial symmetry (circles, regular octagons, regular hexagons, etc.) would be accepted or rejected as possibilities for future testing.

Testing was set up by using a plastic bin of dimensions 34" L x 20" W x 15" H as a "wave tank." One side was marked with one inch increments, and the bin was filled with water to a depth of seven inches (representing an expected testing depth of seven feet). A sheet of acrylic was used to divide the bin in half, which created a narrow channel in order to one-dimensionalize the waves and limit reflection off of the sides. Once the apparatus was set up, a prototype was placed in the water and waves were generated using a wooden mallet. Fig. 2.3.2 shows an image of the testing apparatus. Through research, the team also learned that in addition to scaling prototype dimensions based on Froude number, the generated waves should be scaled based on wave steepness, the ratio of wavelength to wave amplitude (shown in Eq. 2.3.2) [6].

$$\frac{H_p}{l_p} = \frac{H_m}{l_m} \quad (2.3.2)$$

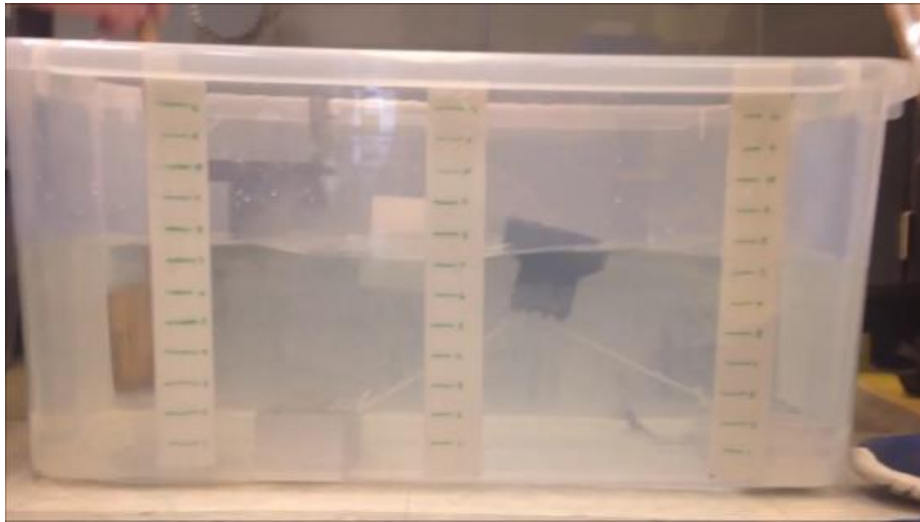


Figure 2.3.2. Side view of the apparatus used to perform prototype testing.

Each trial was video recorded from top and side views in order to be able to go back and see how each prototype pitched and yawed in the water. The Rev 1 and Rev 2 prototypes were tested in this fashion, however once the team was ready to design Rev 3, they determined that it would be pertinent to test the prototypes while they were moored, therefore prototypes Rev 3 and Rev 4 were designed with attachment points so that they could be moored during testing.

From the testing performed on Rev 1, the team determined that the main metrics that they would continue to test for were the ability of the prototype to remain perpendicular to the waves, stability that prevents the prototype from rolling, and conduciveness to pitching motion. The results from the Rev 1 trial showed that the wide upper portion provided excellent stability; however, because the stability was uniform all the way around the shape, the Rev 1 shape severely lacked the necessary pitching motion needed to move the pendulum. Additionally,

without mooring, the prototype was free to rotate, and the circular shape provided no way for it to orient itself perpendicularly to the waves. Moreover, the prototype ended up being too buoyant, so a weight was attached to the bottom of the shape during testing. The deficiencies of Rev 1 led to the changes that resulted in the Rev 2 prototype, shown in Fig. 2.3.3.

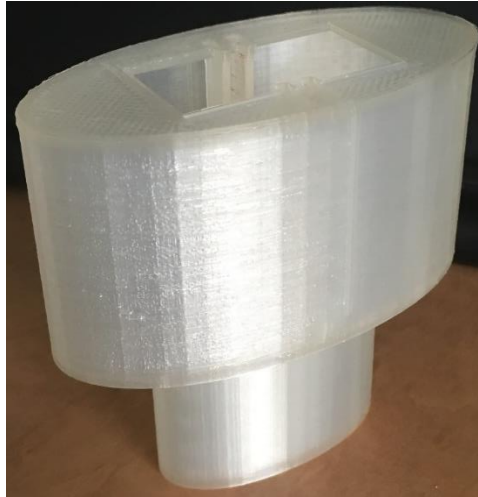


Figure 2.3.3. Rev 2, prototype of external mechanical structure.

The modifications made to Rev 1 that resulted in Rev 2 include changing the shape to have ellipsoidal cross-sections, decreasing the height of the lower compartment, and leaving a hole cut out of the top so that the prototype could be filled with sand that would simulate the weight of the pendulum. The Rev 2 design was able to fix three of the issues observed in the Rev 1 design: the ellipsoidal shape helped the prototype try to orient itself perpendicularly to the incoming waves; the ellipsoidal shape helped the prototype achieve the desired pitching motion; and the hole in the top allowed the team to adjust the weight of the prototype as needed. The major downfall of this design was that it was too top-heavy and therefore not stable enough to prevent itself from rolling. Based on this, the team made more adjustments that ended up resulting in the Rev 3 design shown in Fig. 2.3.4.

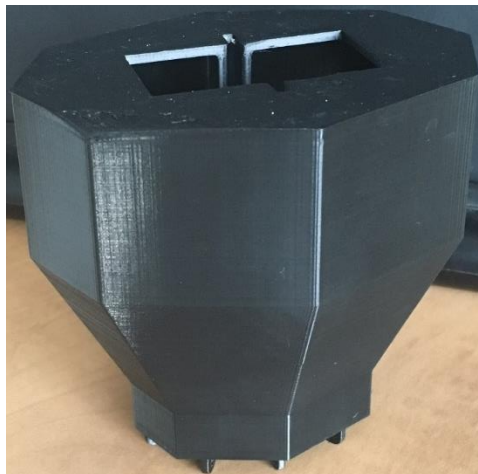


Figure 2.3.4. Rev 3, prototype of external mechanical structure.

This revision included changing the cross-sectional shape to an irregular octagon with ellipsoidal proportions, adding a long chamfer to the outside of the lower compartment and adding the mooring attachments mentioned earlier. This shape change was made in order to more accurately represent a shape that can be easily manufactured for the actual-size WEC. These changes did not noticeably affect the pitching motion of the shape; however, when the prototype was moored to the bottom of the testing tank, it was observed that its pitching motion was slightly impeded. However, the addition of the long chamfer did not help with the stability of the design, so the team decided to make additional changes. These changes yielded the design of Rev 4, the team's current design, which can be seen in Fig. 2.3.5.

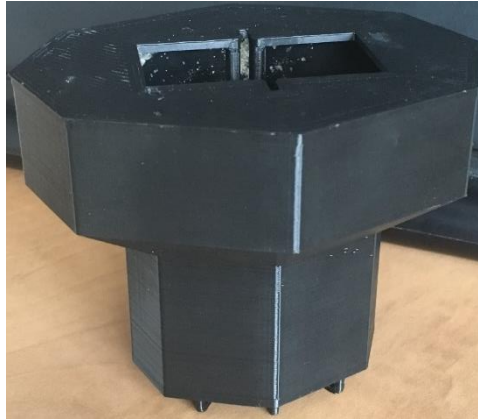


Figure 2.3.5. Rev 4, prototype of external mechanical structure.

In the Rev 4 design, the chamfer was drastically shortened and the height of the upper compartment was decreased. These changes made the design much more stable than the previous two designs but did not visibly decrease the pitching motion or self-orienting performance of the shape, and for this reason, the team has decided on using the Rev 4 design for the preliminary design. Next the team addressed the necessity of developing a mooring method by testing the Rev 4 prototype with different mooring configurations. Testing occurred using the same method as the previous testing. Thus far, a two-point attachment method in which two tethers were attached to the front of the prototype, and a four-point attachment method in which two tethers were attached to each the front and the back of the prototype, have been tested. Figs. 2.3.6 and 2.3.7 show top and side views of the two different mooring methods.

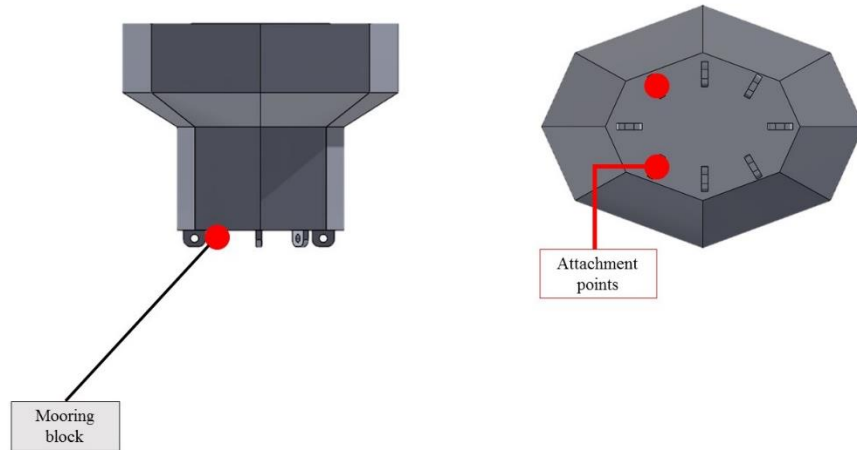


Figure 2.3.6. Side (left) and top (right) views of two-point mooring configuration.

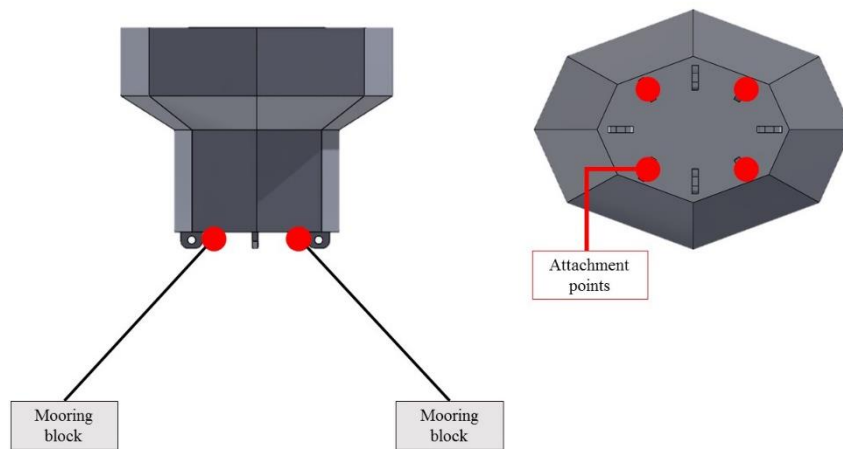


Figure 2.3.7. Side (left) and top (right) views of four-point mooring configuration.

The two-point method allowed the design to retain a large portion of its pitching motion; however, there was no restriction in the back, so the prototype was able to yaw, which is undesirable, as its design is only intended to operate in one direction. The four-point mooring method corrected the excessive yaw issue, but also slightly reduced the prototype's ability to pitch. From these results the team has decided on implementing the four-point attachment method in the preliminary design, but additional configurations will be tested in the future.

2.4 Internal Mechanical Design

ProfWave's internal mechanical design encompasses the pendulum, the internal layout, and structurally linking the exterior hull and all of the internal components. As described above, the pendulum can typically be designed as either a standard pendulum or an off-center weighted circular shape. To combine aspects of both, ProfWave's pendulum was designed as a circular segment, as shown in Fig. 2.4.1.



Figure 2.4.1. SolidWorks rendering of pendulum and cylinders.

This circular segment design is both effective and efficient: in addition to concentrating most of the pendulum's mass in its lower half, it also reduces the amount of unnecessary and undesirable material used, since any mass above the pendulum's center of rotation only opposes the pendulum's natural motion and acts against the system.

The internal structure was divided into two separate levels, shown in Fig. 2.4.2. Each level's mounting plate shape – octagonal for this preliminary design – was sized differently to fit inside the exterior hull at its designated vertical location.

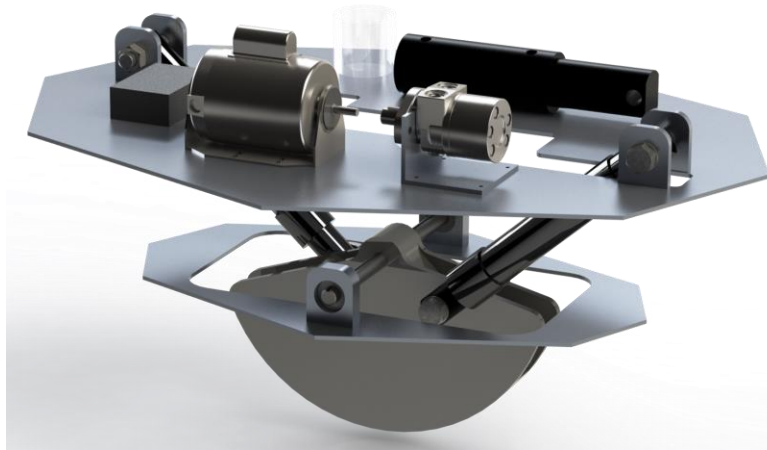
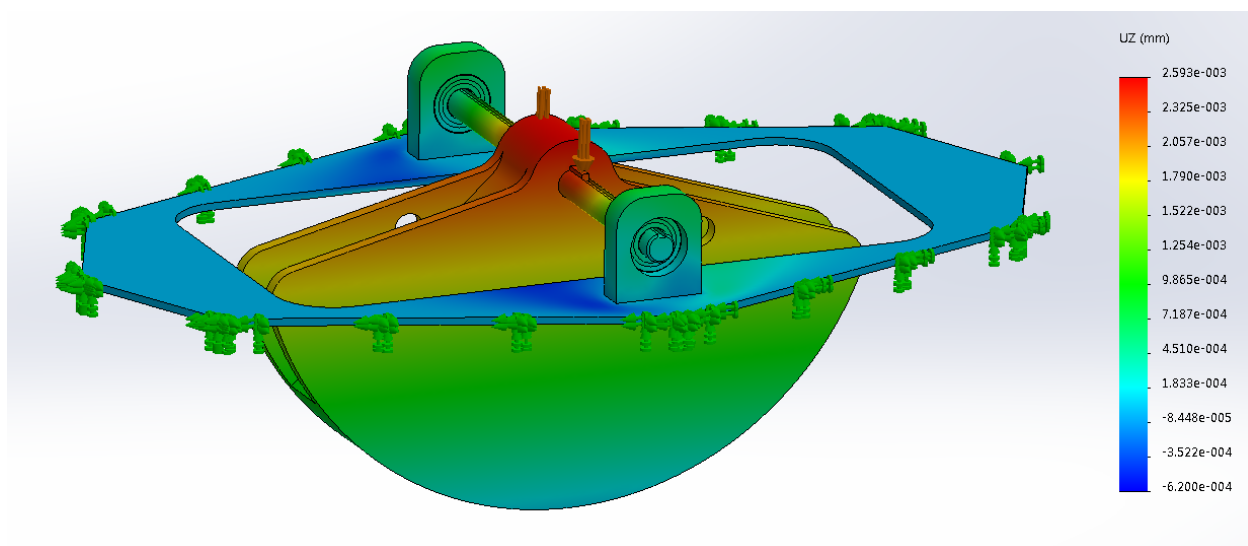


Figure 2.4.2. SolidWorks rendering of the bottom and top levels.

The bottom level's sole purpose is to support the pendulum, since the pendulum is the preliminary design's single heaviest component. In this design, the pendulum is supported by a steel keyed shaft and two double shielded ball bearings (to resist dust and other contaminants), each of which is pressed into a bearing block that is then fixed to the bottom level mounting plate. To verify that none of these components will fail under the weight of the pendulum, a static load analysis was performed on them in SolidWorks. For this analysis, the side edges of the mounting plate were fixed to mimic real conditions, since the plate's edges will not be able to

deflect vertically once it is fastened to the exterior hull. Typically, gravitational forces would simply be turned on in the analysis to simulate the load; however, doing so caused the analysis to continuously return a boundary condition error. As a result, a downward load equal the pendulum's weight was applied along the length of the shaft key. The key was chosen as the area of load application because it provided a similar load distribution to the distributed weight of the pendulum. Applying the load elsewhere – at a singular point, for example – had the potential to increase stress concentrations at that point, which may not provide accurate results. The analysis was run using the finest mesh generated by SolidWorks, to improve accuracy, and the vertical deflection results of all components are shown in Fig. 2.4.3. These results show a maximum vertical deflection on the order of 0.0026 mm, which is effectively negligible and suggests that the bottom level and all of its components can support the weight of the pendulum. A more intensive analysis will be performed for the final design, in which the gravity issue will be resolved, all fasteners will be included, bearing settings will be included, and all local fixtures and relationships between parts will be defined to closely match the real setup. By performing such a detailed analysis, the team will be able to accurately ensure not only that the pendulum's weight can be supported, but also that the bearings or fastener threads will not fail.



2.4.3. Results of SolidWorks load analysis of the bottom level.

Above the bottom level, the upper level supports all of the WEC's other internal components. This includes the hydraulic cylinder end mounts, PTO components – accumulator, hydraulic motor, electric motor, oil reservoir – and the electronics for the on-board data acquisition system. Closer examination of the upper level in Fig. 2.4.2 reveals a channel that has been cut out of the center of the upper level mounting plate. This was done to accommodate the possibility of a full pendulum revolution. While such an occurrence is unlikely, including this channel is a small sacrifice to ensure that a full revolution does not damage – or in a worst case scenario, destroy – the system during operation. Unlike with the bottom level, the combined weight of the upper level's components is not nearly as high as that of the pendulum, so a load analysis on the upper level for the preliminary design was not deemed necessary. However, because the upper level

mounting plate's central channel does introduce stress concentrations and potential new points of failure, a complete analysis will be performed for the final design.

2.5 Power Take-Off System

The power take-off (PTO) system is essentially responsible for converting as much of the pendulum's rotational energy into electrical energy as possible. Mechanical, hydraulic, and electromagnetic power transmission systems were considered, but hydraulic was deemed most suitable for this design. Hydraulic systems tend to use fewer moving parts than mechanical systems, making them simpler and easier to maintain. The few parts that are needed are likely to be purchased—rather than machined by hand—which reduces the likelihood of losses due to less-than-professional manufacturing. Despite needing to purchase most of the parts, a hydraulic system will still be less costly than an electromagnetic system, as magnets of the size required for this application are prohibitively expensive.

The designed hydraulic PTO system consists of two single-acting hydraulic cylinders, a double-acting hydraulic cylinder serving as a hydraulic accumulator, a fixed-displacement hydraulic motor, an electrical DC motor, a working fluid reservoir, one-way check valves, and tubing. When the WEC is hit with a wave, the pendulum inside is designed to swing back and forth. As the pendulum swings in one direction, it compresses the fluid in one cylinder and draws fluid into the other. The opposite happens as the pendulum swings back in the other direction. The displaced fluid travels first through check valves, and then through the hydraulic motor. The hydraulic motor then spins an electrical DC motor in reverse, which acts as an electrical generator. The fluid continues into a reservoir, where it is stored until it is again drawn into the hydraulic cylinders. Ideally, the flow into the hydraulic motor should remain nearly constant. However, the pendulum will displace two relatively large volumes of fluid right after its initial rotation back and forth, and then the displacements will be relatively small as the pendulum oscillates with decreasing amplitude while waiting for another wave collision. To smooth the flow rate, a double-acting cylinder will be placed in the system between the driven cylinders and the hydraulic motor to act as an accumulator. The cylinder will be charged with pressurized air on one side and fluid on the other. During the large displacements, excess fluid will be stored in the accumulator. It will then be released to supplement the flow through the hydraulic motor during periods of small displacements. A schematic of the PTO system is shown in Figure 2.5.1.

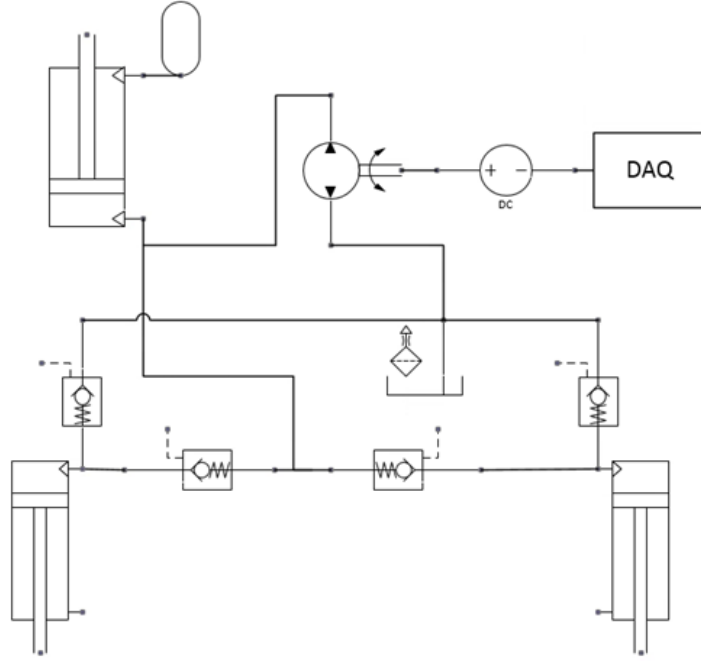


Figure 2.5.1. PTO schematic.

To calculate the power extracted from the hydraulic motor, a simple energy balance calculation was performed.

$$E_{IN} - E_{OUT} + E_{GEN} = \frac{dE_{ST}}{dt} \quad (2.5.1)$$

There is no energy generated internally, and steady state is assumed, so both of these terms become zero.

$$\dot{m}_{IN} \left(\frac{v_{IN}^2}{2} + gz_{IN} + u_{IN} + \frac{P_{IN}}{\rho_{IN}} \right) - \dot{m}_{OUT} \left(\frac{v_{OUT}^2}{2} + gz_{OUT} + u_{OUT} + \frac{P_{OUT}}{\rho_{OUT}} \right) + \dot{Q}_{IN} - \dot{W}_{OUT} = 0 \quad (2.5.2)$$

Next, it is assumed that there is either zero or negligible change in fluid velocity, height, internal energy, and density. It is also assumed that there is no heat transfer within the control volume and the mass flow rate in is equal to the mass flow rate out.

$$\dot{W}_{OUT} = \dot{m} \left(\frac{P_1}{\rho} - \frac{P_2}{\rho} \right) \quad (2.5.3)$$

Mass flow rate is equal to the product of density and volumetric flow rate, \forall .

$$\dot{W}_{OUT} = \rho \forall \left(\frac{P_1}{\rho} - \frac{P_2}{\rho} \right) \quad (2.5.4)$$

Cancelling the density values and replacing P_1 with $P_{Operating}$ and P_2 with $P_{Atmospheric}$ provides the following equation:

$$\dot{W}_{OUT} = \forall (P_{Operating} - P_{Atmospheric}) \quad (2.5.5)$$

Our extracted power is therefore equal to the product of volumetric flow rate and the change in pressure. If pressures are converted to gauge rather than absolute pressures, the equation can be rewritten as shown:

$$\dot{W}_{OUT} = (\forall)(P_{Operating}) \quad (2.5.6)$$

Due to space and cost constraints, hydraulic snow plow cylinders with two-inch bores and ten-inch strokes were selected to be driven by the pendulum, with the intention of sizing the remain components off of them. The original plan was to purchase a 33-ounce threaded diaphragm accumulator. However, the operating pressure ranges likely to be achieved by the PTO system are far too low for the use of an industrial accumulator. These accumulators require minimum operating pressures of around 300 psig. Instead, a double-acting cylinder with a three-inch bore and ten-inch stroke was selected. By pre-charging one side of the cylinder with pressurized air, the other side of the cylinder will be able to store and release fluid as needed to smooth the fluid flow rate into the hydraulic motor. Unfortunately, without a completed dynamics model, the force acting on the fluid from the driven cylinders cannot be determined. This makes accurately sizing a hydraulic motor and electrical generator impossible at the current time. Still, it is worth making an attempt to estimate power production using conservative estimation. Assuming only quarter-stroke displacement in each cylinder gives a displaced volume of 15.7 in³. Using wave data collected from SwellInfo.com (see Appendix) on the waters surrounding Pierce's Point, a conservative time interval of ten seconds between wave occurrences can be estimated. This provides an average volumetric flow rate of 1.57 in³/s. Assuming a 50-pound force is applied to each driven cylinder by the pendulum, this produces an operating pressure of 15.9 psig. The product of volumetric flow rate and operating pressure produces an estimated power output of nearly 25 in-lbf/s, or 2.8 Watts. This value appears to be in the realm of feasibility, as a commercial prototype of similar scale built in France during the early 2000s achieved comparable results (approximately 6 Watts) [7].

2.6 Electronics and Data Acquisition

As previously mentioned, the primary metric for success of the WEC is net-positive power production. In order to accurately measure the power output of the WEC and gather relevant metrics on the performance and behavior of the system, a data acquisition system was included in the ProfWave design. There were two metrics to be considered in the design of the data acquisition module for ProfWave: power output; and accelerometer data from the center of mass of the pendulum and center of mass of the entire WEC.

The first major decision to be made in the design of the data acquisition system was what controller to use. Three main options were considered: Arduino Uno, Texas Instruments MSP430F551, and the Raspberry Pi 3 Model B. The metrics considered to be the most important

in deciding on a controller were: the language which is used to program the device; the number of General Purpose Input Output (GPIO) pins; the cost; the amount of internal storage; the availability of adding external storage via a micro-SD card; and potential wireless capability. Table 2.6.1 shows the comparison between the three microcontroller options in these critical metrics.

Table 2.6.1. Comparison of controller options considered in the design of ProfWave's DAQ unit.

| <i>Controller</i> | <i>Arduino Uno</i> | <i>MSP430F551</i> | <i>Raspberry Pi 3 Model B</i> |
|-------------------------|--------------------|-------------------|---------------------------------|
| <i>Language</i> | Modified C/C++ | C | Python |
| <i>GPIO Pins</i> | 14 | 47 | 40 |
| <i>Cost</i> | \$22 | \$13 | \$40 |
| <i>Internal Storage</i> | 32KB | 128KB | 1GB |
| <i>SD Card?</i> | External Module | External Module | Built in Micro-SD |
| <i>Wireless?</i> | External Module | External Module | Bluetooth 4.1 + 802.11 Wireless |

Based on the research performed on the selected controller options, the Raspberry Pi 3 Model B was chosen. The reasoning for this decision lies in the Raspberry Pi 3 Model B's vastly superior internal storage and integrated micro-SD card reader. This is important to ensure that a sufficient amount of sensor data can be collected to draw meaningful conclusions without reaching the limits of the device and for ease of use, as adding a micro-SD card reader to the Arduino would take up the limited GPIO pins and adding a micro-SD card to the MSP430 would require a significant amount of additional work in both code and fabrication of a PCB interface when compared to the relative ease of using the Raspberry Pi. Additionally, the Raspberry Pi 3 Model B comes with built-in Bluetooth 4.1 capability which would allow for a potential wireless local connection to be established between ProfWave and a Bluetooth-capable device to pull live data from the WEC in operation.

In order to measure the power output of the WEC, the simplest solution is to measure the voltage, V , across a load resistor, R_L . The power can then be calculated according to Eq. 2.6.1.

$$P = \frac{V^2}{R_L} \quad (2.6.1)$$

In order to record the voltage data on the controller, an Analog to Digital Converter (ADC) is needed to take the analog voltage value and deliver a serial 16-bit binary value representing the voltage at both ends of the resistor. The Adafruit ADS1115 16-Bit ADC was chosen because the availability of Python libraries used to communicate with the Raspberry Pi using I²C (Inter-Integrated Circuit) communication protocol. A simplified schematic showing the power measurement scheme is shown in Fig. 2.6.1.

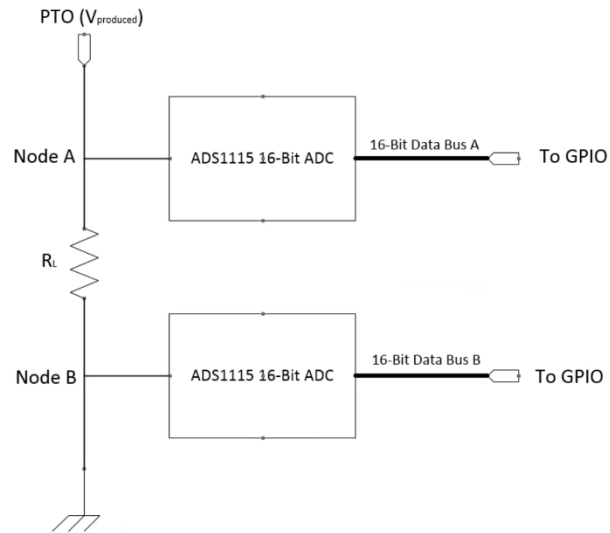


Figure 2.6.1: Schematic showing the configuration used to measure power output from the WEC.

In addition to the ADC, an accelerometer was added to the design in order to gather data on the motion of the pendulum and the motion of the WEC as a whole. These locations are shown in Fig. 2.6.2.

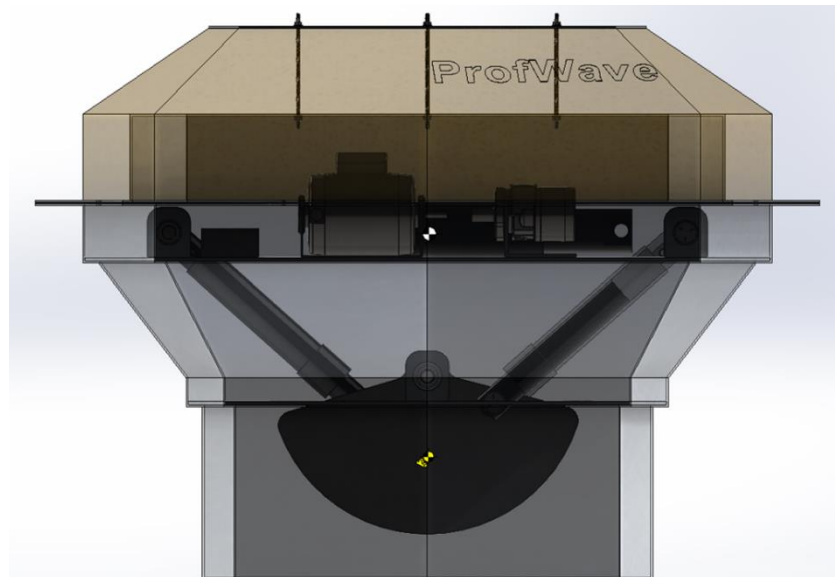


Figure 2.6.2. SolidWorks model with called-out pendulum and WEC centers of mass.

There is a gap in the literature about this buoy-pendulum design regarding the relationship between the motion of the center of mass of the pendulum and the center of mass of the buoy. For this reason, ProfWave presents an opportunity to expand on the research of WEC systems – and wave modeling in general – if a meaningful relationship can be discerned. Also, the accelerometer data can be used to verify the accuracy of wave simulation software and potentially find ways of improving the accuracy of the simulations. The accelerometer, as with the ADC before, was chosen such that the model would be easily compatible with the Raspberry

Pi and a Python library was available for interfacing with the accelerometer. Based on these criteria, the Adafruit ADXL345 Digital Accelerometer was chosen, as it fits all of the specified requirements. In order to achieve a redundant design and to verify and validate the accelerometer data, two accelerometers will be placed as close to the center of mass of both the WEC and the pendulum. The GPIO pin-out of the Raspberry Pi 3 Model B and the connection configurations of the ADS1115 and ADXL345 can be found in the Appendix.

3 Technological Impact Statement

3.1 Societal Impact

Research into sustainable forms of power generation continues to become increasingly important from year-to-year. The need to reduce dependence on non-renewable fossil fuels to power the grid presents a both challenging and urgent engineering problem for the next generation of scientists and engineers. It may be difficult to gauge the lasting societal impact of a small-scale project like ProfWave on the field of renewable energy, but analysis of the performance of ProfWave will present a unique opportunity to contribute to renewable energy research. The design of ProfWave was specifically picked due to the limited amount of research being done on this buoy-pendulum power generation scheme in WEC. Additionally, the data collected to analyze the movement of the buoy-pendulum system while the WEC is in operation can be used to verify the accuracy of ocean wave modeling software and may present a unique opportunity for the ProfWave team to contribute meaningful research to the simulation of ocean waves and improve the accuracy of modeling software.

3.2 Environmental Impact

The use of a hydraulic PTO system in a marine application presents the risk of hydraulic fluid leaking into the water, potentially damaging the local ecosystem. To eliminate this risk, an environmentally friendly, biodegradable hydraulic fluid based upon rapeseed (canola) vegetable oil will be used.

3.3 Manufacturability

Prototyping is always an integral part to any design project, but it is especially so in a project like ProfWave, where the central concepts have not been extensively researched. The different subsystems within this WEC each require their own form prototyping, whether it be for experimental design or proof of concept, but at the project's current stage of development, it was only possible to prototype the external structure of the WEC. When deciding how to prototype the outer structure, the team weighed three main options: the first option was to have models CNC machined out of aluminum; the second option was to machine the prototypes by hand; and the third option was create the prototypes using a 3D printer. The team ultimately decided on the 3D printing option because, while metal prototypes would be closer to a true scaled model (in terms of weight) and they would look nicer, machining the prototypes out of metal would be impractical and time-consuming. The team does not have the skills necessary to machine the prototypes by hand and using a block of metal for each prototype would be an unnecessary use of material and money. 3D printed parts can be made with comparable accuracy, less material, and fewer expenses than machined parts, so the team decided to go with this option.

When designing the prototypes, efforts were made to optimize the parts for low printing time and low material use, while still maintain good quality. This was made possible because one of the team members worked extensively with 3D printers and 3D printed parts at a summer internship. Specific design and printer setting choices were as follows: parts were modeled as hollow bodies instead of solid bodies; parts were designed to be printed with a specific extruder nozzle size; parts were oriented in a specific manner in Cura. These choices optimized the printing process because, in some combination, they gave the designer finer control over thickness and layer height, so the designer was able to eliminate partial passes (when the nozzle is not pushing out a full nozzle width of material) and minimize the number of layers necessary to print a sturdy, good quality part. These choices also eliminated the need for support material inside or outside the part, which saved printing time and material.

Included in the process of designing the external structure of the WEC, a short materials analysis was conducted. The main materials considered for the external structure were sheet aluminum, sheet steel, and sheet plastic. Considering the fact that the structure would need to support between 200 and 350 pounds of internal parts, the team determined that one of the two metals would be able to better provide the necessary durability. From there, the operating environment was considered. Most of the potential testing locations that the team has been looking into are salt water bodies, thus oxidation- and corrosion-resistance are qualities that the external structure will need. Steel oxidizes more readily than aluminum and aluminum is lighter than steel, which would make the final product easier to transport. Therefore the team has selected sheet aluminum as the external structure material for the preliminary design. In addition to investigating different materials, the team also began to look into different foams to provide additional buoyancy, epoxy resin to provide water proofing, and anti-corrosion treatments to prevent the salt from corroding the structure; however, no final decisions have been made on these fronts yet.

Most of the parts required for the PTO system will likely be purchased from online vendors, such as McMaster-Carr and Surplus Center. Parts like hydraulic cylinders and motors require precise machining in order to maintain tolerances that prevent fluid from leaking out of the system. Other components, like the electrical motor and check valves, are outside of the team's realm of manufacturing experience. The WEC's other subsystems are already expected to require significant manufacturing, so the team decided that the easily available, high quality, and affordable parts needed for the PTO system should simply be purchased.

4 Conclusion

The idea for ProfWave began in August, and it has since been turned into a successful Junior/Senior Engineering Clinic project. This semester, the project was outlined and initial research into WECs was conducted. At the same time, the team was able to secure a total of \$2,751 for the project. After selecting the buoy-pendulum design, the team investigated the dynamics of the system before actually designing the WEC. A preliminary design for the actual-size WEC was created in SolidWorks, and all internal components have been tentatively selected. The team has also investigated potential testing sites that include Pierce's Point near Cape May, NJ, and the Ohmsett test facility in Leonardo, NJ.

The most immediate next step of the ProfWave project is to either finish writing the dynamics model in MATLAB, or to acquire the ANSYS Aqwa simulation software. Gaining access to the

Aqwa software would be preferable because there is great deal of complex and compounding mathematics that the team has no experience with. If the software can be acquired during the winter break or right at the beginning of the spring semester, the team can quickly work on optimizing the final design. Optimizing the final design for manufacturability, cost, and efficiency, and sizing the remaining components would be the next logical step. Once the design is finalized, the rest of the project falls into place because all that will remain will be to order parts, fabricate the WEC and put it out in the water for testing. There is also the potential that more funding will be needed, but that is a decision that will be made once the team has finalized the design and has a complete bill of materials. If more funding is required, the team plans to submit an application to the spring campaign of PROffunder and to seek out external sponsorships. The team is also planning to evaluate the workload (specifically in fabrication and manufacturing) for the spring semester, in order to decide whether or not the project will require additional team members.

5 Acknowledgments

The team would like to specifically thank the following individuals and organizations who have helped ProfWave transform from a simple idea into a fully-fledged, funded project:

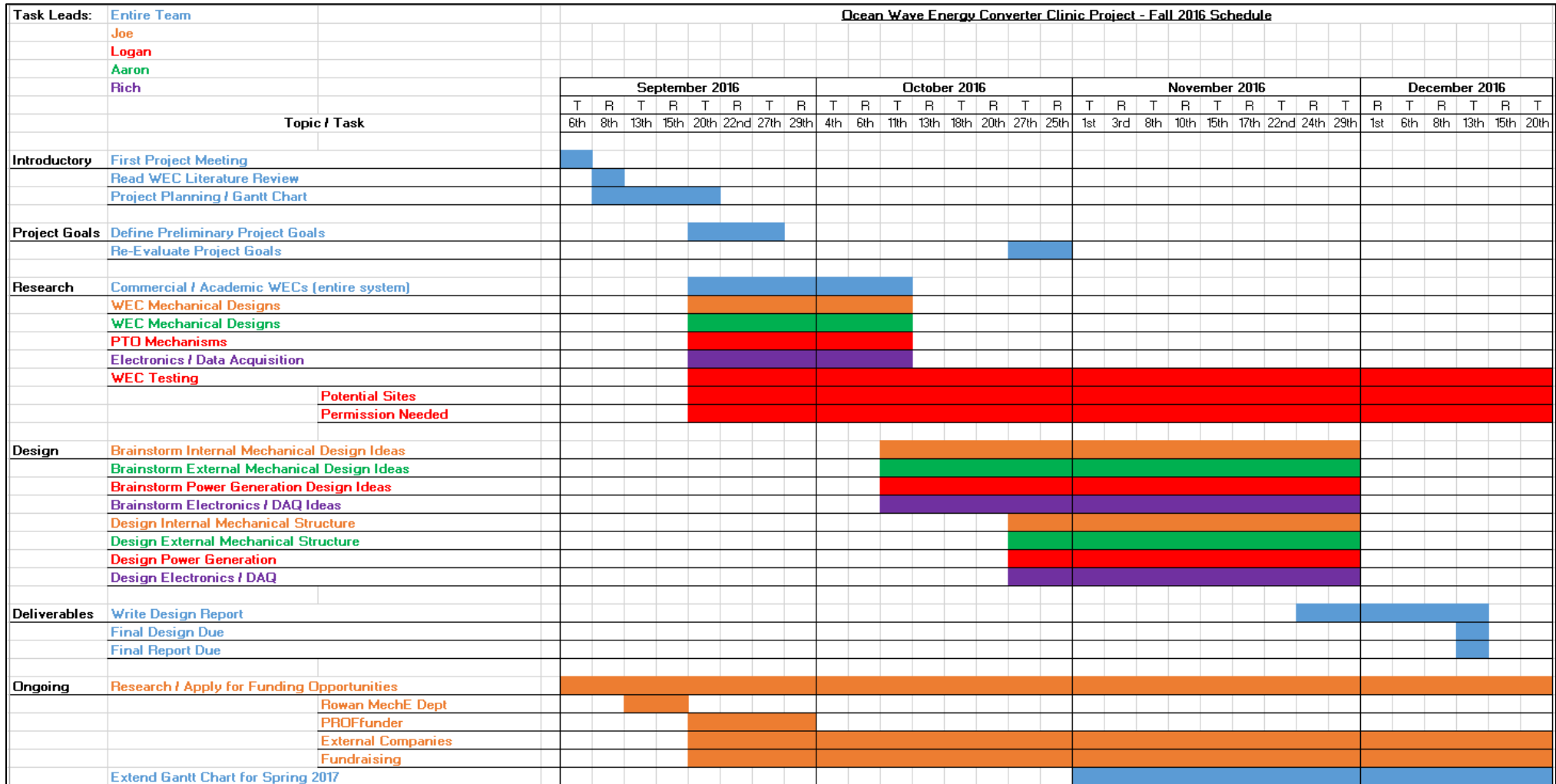
Dr. Kaitlin Mallouk, ProfWave's faculty advisor,
Dr. Eric Constans, our dynamics consultant,
Dr. Krishan Bhatia, our hydraulic systems consultant,
Brighid Burgin and Alan Ford, our PROffunder Alumni Sponsors,
The Rowan University Mechanical Engineering Department,
The Rowan University Alumni Association and all of the project's PROffunder donors.

6 References

- [1] H. Polinder and M. Scuotto. "Wave Energy Converters and Their Impact on Power Systems," in *International Conference on Future Power Systems*, November 2015, pp. 1-9. Available: doi:10.1109/FPS.2005.204210.
- [2] A. Clément et al. "Wave Energy in Europe: Current Status and Perspectives." *Renewable and Sustainable Energy Reviews*. vol. 6(5), pp. 405-431, Oct. 2002. Available: doi: 10.1016/S1364- 0321(02)00009-6.
- [3] A. von Jouanne. (2011, March). "Harvesting the Power of the Ocean." *American Society of Mechanical Engineers*. [Online]. Available: <https://www.asme.org/engineering-topics/articles/renewable-energy/harvesting-the-power-of-the-ocean>.
- [4] K. Burman et al. "Ocean Energy Technology Overview." *National Renewable Energy Laboratory*. [Online]. pp. 1-32, July 2009. Available: DOE/GO-102009-2823.
- [5] B. Drew et al. "A Review of Wave Energy Converter Technology." *Proc. Institution of Mechanical Engineers, Part A: Journal of Power and Energy*. vol. 223(8), pp. 887-902, Dec. 2009. Available: doi: 10.1243/09576509JPE782.
- [6] H. Sarlak et al. "Experimental Investigation of Offshore Wave Buoy Performance." *Journal of Mechanical Engineering*, vol. 6(11), Spring & Summer 2010. [Online].
- [7] J. Cordonnier et al. "SEAREV: Case study of the development of a wave energy converter." *Renewable Energy*. vol. 80, pp. 40-52, Aug. 2015. Available: doi: 10.1016/j.renene.2015.01.061

7 Appendix

7.1 Fall 2016 Project Gantt Chart



7.2 Wave Data Collected for Pierce's Point, NJ

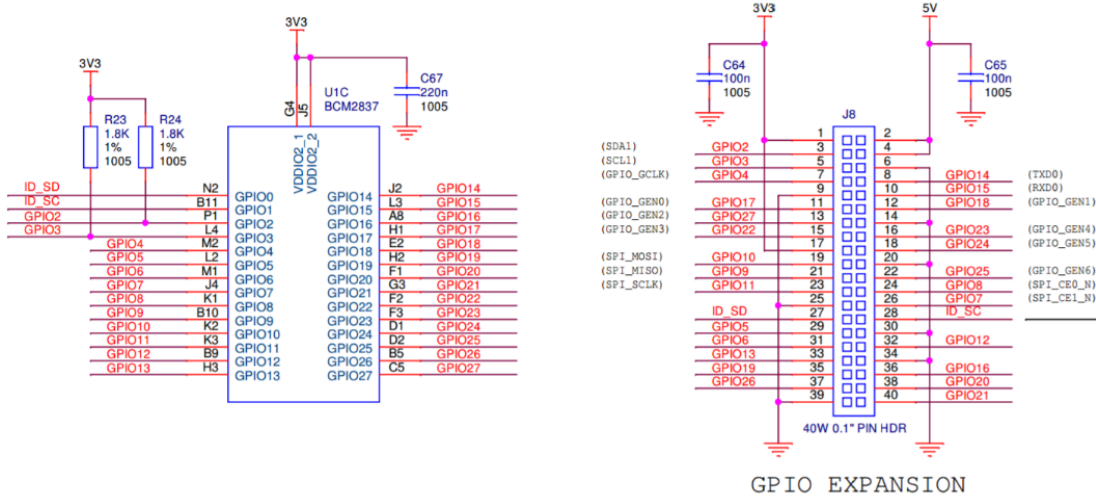
Pierce's Point Wave Data

Source: SwellInfo.com

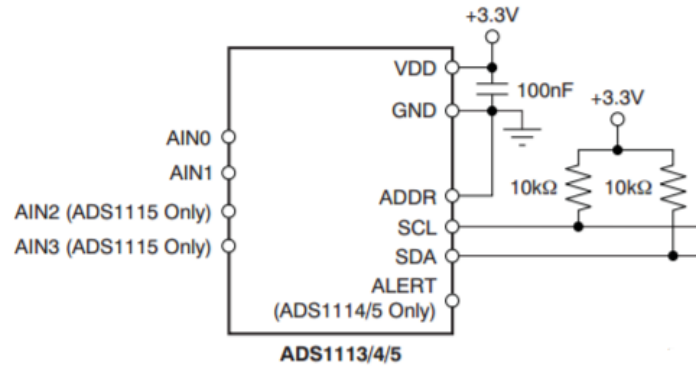
Daily surf reports for Pierce's Point, NJ

| Date | Swell | Period |
|-------------|--------------|---------------|
| 11/8/2016 | 0'-2' | 13 sec |
| 11/9/2016 | 0'-2' | 10 sec |
| 11/10/2016 | 1'-2' | 10 sec |
| 11/11/2016 | 0'-2' | 9 sec |
| 11/12/2016 | 0'-1' | 3 sec |
| 11/13/2016 | 0'-1' | 10 sec |
| 11/14/2016 | 1'-2' | 9 sec |
| 11/15/2016 | 1'-2' | 8 sec |
| 11/16/2016 | 1'-2' | 8 sec |
| 11/17/2016 | 1'-2' | 7 sec |
| 11/18/2016 | 1'-2' | 9 sec |
| 11/19/2016 | 1'-2' | 10 sec |
| 11/20/2016 | 2'-3' | 10 sec |
| 11/21/2016 | 0'-1' | 5 sec |
| 11/22/2016 | 0'-1' | 4 sec |
| 11/23/2016 | 0'-1' | 7 sec |
| 11/24/2016 | 0'-1' | 9 sec |
| 11/25/2016 | 0'-1' | 9 sec |
| 11/26/2016 | 0'-1' | 10 sec |
| 11/27/2016 | 0'-1' | 9 sec |
| 11/28/2016 | 0'-1' | 8 sec |
| 11/29/2016 | 3'-4' | 6 sec |
| 11/30/2016 | 2'-3' | 8 sec |
| 12/1/2016 | 2'-3' | 8 sec |
| 12/2/2016 | 1'-2' | 7 sec |
| 12/3/2016 | 0'-1' | 5 sec |
| 12/4/2016 | 0'-1' | 3 sec |
| 12/5/2016 | 1'-2' | 7 sec |
| 12/6/2016 | 2'-3' | 8 sec |
| 12/7/2016 | 2'-3' | 8 sec |
| 12/8/2016 | 1'-2' | 7 sec |
| 12/9/2016 | 0'-1' | 8 sec |
| 12/10/2016 | 0' | 0 sec |
| 12/11/2016 | 0' | 0 sec |
| 12/12/2016 | 2'-3' | 7 sec |
| 12/13/2016 | 1'-2' | 7 sec |
| 12/14/2016 | 1'-2' | 7 sec |

7.3 GPIO Pinout of Raspberry Pi 3 Model B



7.4 Connection Diagram for ADS1115 16-Bit ADC



7.5 Connection Diagram for ADXL345 Digital Accelerometer

